Cement and Concrete Research 42 (2012) 173–185

Contents lists available at SciVerse ScienceDirect

Cement and Concrete Research

journal homepage: http://ees.elsevier.com/CEMCON/default.asp

Investigation of the influence of blast-furnace slag on the resistance of concrete against organic acid or sulphate attack by means of accelerated degradation tests

Elke Gruyaert, Philip Van den Heede, Mathias Maes, Nele De Belie *

Magnel Laboratory for Concrete Research, Ghent University, Department of Structural Engineering, Technologiepark Zwijnaarde 904, B-9052 Ghent, Belgium

ARTICLE INFO

Article history:
Received 20 April 2011
Accepted 20 September 2011

Keywords:
Granulated blast-furnace slag (D)
Organic acids (D)
Sulphate attack (C)
Permeability (C)
$Ca(OH)_2$ (D)

ABSTRACT

Replacement of ordinary Portland cement (OPC) by blast-furnace slag (BFS) alters the durability behaviour of concrete. In this research, the influence of BFS on the concrete's acid or sulphate resistance is investigated by accelerated degradation tests and the results are related to microstructural and physico-chemical parameters.

A significant reduction of acid deterioration was recorded for BFS concrete, which is mainly attributed to the different chemical composition of the binder. General durability indicators like open porosity cannot solely explain the different performances of OPC and BFS concrete. In contrast, the resistance of concrete cyclically and partially submerged in sulphate solutions decreases when high amounts of cement are replaced by BFS. Crystallisation pressure causes more severe deterioration in these cases.

1. Introduction

The testing apparatus for accelerated degradation tests developed by De Belie et al. [1] has been extensively applied in the past to determine concrete's resistance against organic (lactic–acetic acid [2]) and inorganic acids (sulphuric acid [3]). In the current research, not only the acid resistance, but also the sulphate resistance of blast-furnace slag (BFS) concrete is investigated separately by means of this equipment.

For specific fields of application, like agricultural structures (e.g. floors in animal houses and silage structures) or in the food industry, concrete can be exposed to aggressive organic acid attack. Liquid manure is a combination of mainly acetic, propionic, butyric and isobutyric acids while feed acids and silage effluents mainly consist of lactic and acetic acids [4,5]. According to Bertron et al. [4], the four acids in liquid manure are equally aggressive, while lactic acid, present with acetic acid, is more aggressive according to the pK_a value (dissociation constant). The experimental programme of the current research project focuses on degradation of concrete exposed to lactic–acetic (CH_3–CHOH–COOH and CH_3–COOH) acid solutions. Although both are weak acids ($pK_a = 3.86$ for lactic acid and $pK_a = 4.75$ for acetic acid), the acceptable pH limits without exaggerated degradation are higher than for strong acids: the acid concentration of weak acids is much higher than that of strong acids to obtain the same pH level and weak acids are thus more aggressive for a given pH [6]. The reaction mechanism with hydrated phases in ordinary Portland cement (OPC) concrete can be summarised as follows: calcium hydroxide (CH), which is the most vulnerable phase towards acid attack, in concrete reacts with the lactic–acetic acid and produces soluble calcium salts (calcium lactate and calcium acetate). When these salts leach from the concrete, the porosity increases, the pH level in the pores drops and cement hydrates gradually become unstable. The end result is a total disintegration of the material [4,5,7].

According to De Belie et al. [5], three factors seem to play an important role in the acid resistance of concrete: (i) the permeability, determining the extent to which acids can penetrate into concrete, (ii) the alkalinity and (iii) the chemical composition of the cement paste. Previous studies have shown the positive influence of mineral additions, such as fly ash (FA) [4,7], silica fume (SF) and blast-furnace slag (BFS) [8,9] because of the lower CH content, reduced Ca-to-Si (C/S) ratio in calcium silicate hydrates (C–S–H) and the refined pore structure they produce in concrete [4,5]. In [10], concrete containing CEM III (blast-furnace slag cement) showed the best resistance against lactic–acetic acid attack, followed by CEM II (pozzolanic cement), CEM V (composite cement) and CEM I (Portland cement). From the work performed by Bertron et al. [8,11], it seemed that cement pastes made with CEM III/B 42.5 N and exposed to synthetic liquid manure (pH 4 or pH 6) also performed better than OPC pastes. The mass loss and the altered depth were less for BFS pastes. Nevertheless, the altered zone in BFS paste as well as in OPC paste showed an almost complete decalcification and disappearance of crystallised (anhydrous and hydrated compounds) and amorphous hydrated phases. Moreover, the zone consists almost completely of Si, Al and Fe and has a poor mechanical performance, but the probable formation of silica gel containing Al and Fe limits the kinetics of further

* Corresponding author. Tel.: +32 9 264 55 22; fax: +32 9 264 58 45.
E-mail address: Nele.Debelie@UGent.be (N. De Belie).

0008-8846/$ – see front matter © 2011 Elsevier Ltd. All rights reserved.
doi:10.1016/j.cemconres.2011.09.009

alteration. Finally, for the solutions with a pH of 4 (and not for those with a pH of 6), a slight decalcification of the anhydrous slag particles could be observed. From different articles published by Bertron et al. [4,8] it seems that cements containing a high amount of SiO_2, a low amount of CaO and high amounts of e.g. Fe_2O_3 and Al_2O_3 are more resistant to acid attack.

The ingress of sulphates in concrete structures can also cause severe deterioration (cracking, spalling, increased permeability and strength loss) because of chemical and physical processes.

(i) The chemical reactions between sulphates and hydrated cement components yield the following reaction products [12]: secondary gypsum ($CaSO_4.2H_2O$), secondary ettringite ($3CaO.Al_2O_3.3CaSO_4.32H_2O$), thaumasite ($CaSiO_3.CaSO_4.CaCO_3.15H_2O$), brucite ($Mg(OH)_2$), M–S–H ($3MgO.2SiO_2.2H_2O$) and silica gel ($SiO_2.xH_2O$). Secondary ettringite formation causes expansion and cracking. Whether gypsum formation results in expansion is disputed in the literature [13]. El-Hachem et al. [14] and Santhanam et al. [15] mention that ettringite as well as gypsum have an expansive and destructive character, while others [16] claim that the contribution of gypsum is limited while the expansion of ettringite dominates. Thaumasite formation leads to strength loss due to the decomposition of the strength-forming hydration products (C–S–H) [17]. In case of $MgSO_4$ attack, brucite forms a protective layer on the surface, which slows down the degradation process. However, as the attack progresses (due to diffusion of sulphate ions through this layer), the formation of gypsum and ettringite, underneath this layer, leads to expansion, strength loss and cracking of the brucite layer. Finally, C–S–H is converted to M–S–H, which leads to softening of the material [18–22].

(ii) A literature review concerning the mechanisms of physical sulphate attack can be found in the work of Liu [12]. Only the findings which are important for the current research are described below:
- *Salt crystallisation pressure cannot occur in the pores of hydrated cement paste*: Because of the chemical adsorption (attraction) between the main hydrated phases (C–S–H and CH) and the salts, no film of solution can be formed between the pore wall and the crystal. This film is however an essential factor to build up the crystallisation pressure since it allows the solute to diffuse to the crystal which is growing. If no film is present, a growing crystal (which could be nucleated as the energy barrier was exceeded because of alternating conditions) comes into contact with the pore wall, the growth stops and no crystallisation pressure is developed.
- *Crystallisation may occur in completely carbonated cement paste*: Since there is no chemical adsorption between the salts and $CaCO_3$, the aqueous film can be formed between the pore wall and the crystal and crystallisation pressure can be built up.
- Crystallisation of salts only occurs in concrete structures which are *partly* exposed to sulphate solutions: one part of the structure is exposed to a relatively dry air, while another part is in direct contact with water or sub-surface water containing sulphates.

Different studies indicate that the addition of BFS can significantly improve the sulphate resistance. This phenomenon is attributed to the reduced permeability and the different chemical compositions of the binder. According to the appendix *X*2 of ASTM C 989-06, which deals with the effect of slag on sulphate resistance, replacement of cement by BFS reduces the C_3A content of the material and decreases the CH content and the permeability of the mortar/concrete. Brown et al. [23] showed that the replacement of cement by slag reduces the degradation due to sulphate attack and attributed this positive effect to the dense microstructure. The length change and penetration depth of sulphates in BFS concrete with slag/binder (s/b) ratios of 0.45 and 0.72 were significantly reduced in comparison to OPC concrete and even in comparison to concrete containing blast-furnace slag cement (ASTM V), but no significant differences could be found between both BFS concrete mixtures. While Brown et al. [23] showed the effectiveness of BFS in the case of Na_2SO_4 and $MgSO_4$ solutions, other researchers like Higgins [19] and Taylor [24] mentioned a higher effectiveness of BFS in case of Na_2SO_4 solutions. Rozière et al. [25], who investigated the sulphate resistance of mortars with a s/b ratio of 0.62 (slag cement but also separate addition of BFS) according to ASTM C 1012 (Standard Test Method for Length Change of Hydraulic-Cement Mortars Exposed to a Sulfate Solution), also recorded a reduced expansion in comparison to OPC mortar. Contrarily, other studies show that the effect of additions is not always positive. It depends on the alumina content (the lower the content, the higher the resistance) [24] and the degree of immersion [12]. It seems that BFS concrete which is completely immersed in the sulphate solution performs better than OPC concrete, while the reverse is the case for partial immersion [12]. The part of the concrete which was not immersed suffered most from sulphate degradation (mainly salt crystallisation). Although slag cements are generally classified as high sulphate resistant cements, it is demonstrated in [22] that under conditions promoting thaumasite formation (and without considering the permeability of the microstructure), slag cements are accompanied by more intensive thaumasite formation than Portland cements.

2. Materials and methods

2.1. Mix design

2.1.1. Concrete

To compare OPC concrete with BFS concrete, mixes were made in which 0 mass% (S0), 50 mass% (S50), 70 mass% (S70) and 85 mass% (S85) of the cement were replaced by BFS. The water-to-binder ratio (w/b) was 0.5 and the compositions for 1 m^3 concrete are in Table 1. CEM I 52.5 N, complying with the European Standard EN 197-1 (2000), was used and the slag was added to the concrete mix as a separate component. The characteristics of the cement and slag are summarised in Table 2. Because cement quality is degrading with time, different batches of cement (OPC(I), OPC(II) and OPC (III)) and slag (BFS(I), BFS(II) and BFS(III)) were used during this research project. The differences in chemical composition are however very limited.

The test specimens were stored in a curing room at a temperature of 20 °C and a R.H. higher than 95% until the time of testing.

2.1.2. Cement paste

Thermogravimetric measurements were performed on pastes, made with a w/b ratio of 0.5 and s/b ratios of 0% (S0(CP)), 30% (S30(CP)), 50% (S50(CP)) and 85% (S85(CP)). To avoid segregation and bleeding, the mixes were cast in cylindrical rotating moulds (ø 46 mm; h 50 mm) and stored in a climate room at 20 °C and 60% R.H. After 1 day, the specimens were cured in a water bath at (20 ± 2) °C.

Table 1
Concrete composition of S0, S50, S70 and S85 (kg/m^3 concrete) together with the mean value and standard deviation of the 28-day compressive strength (N/mm^2).

	S0	S50	S70	S85
OPC	350	174	105	52
BFS	0	174	244	295
Water	175	174	174	174
Dredged siliceous sand 0/4	791	788	787	785
Gravel 2/8 (rounded)	425	423	423	422
Gravel 8/16 (rounded)	618	616	615	614
28-day compressive strength (OPC (II), BFS (II))	51 (±3.5)	44 (±3.3)	38 (±2.6)	32 (±4.1)

Table 2
Chemical composition (%) and Blaine fineness (m^2/kg) of the Portland cement and blast-furnace slag.

	OPC (I)	OPC (II)	OPC (III)	BFS (I)	BFS (II)	BFS (III)
CaO	62.21	63.12	63.37	40.38	42.64	41.24
SiO_2	18.84	18.73	18.90	34.35	33.86	36.37
Al_2O_3	5.39	4.94	5.74	11.36	8.91	9.83
Fe_2O_3	3.79	3.99	4.31	0.48	0.69	0.26
MgO	0.86	1.02	0.89	7.57	7.39	7.41
K_2O	/	/	0.73	0.37	0.52	0.41
Na_2O	/	/	0.47	0.29	0.28	0.28
SO_3	3.06	3.07	3.34	1.65	1.62	1.62
S^{2-}	/	/	/	0.77	0.72	0.79
CO_2	0.72	0.65	0.50	0.25	0.36	0.90
Mn	/	/	/	0.17	0.19	/
Cl^-	/	/	/	0.01	0.01	0.02
Insoluble residue	0.25	0.21	0.41	0.05	0.16	0.43
LOI[a]	1.65	2.12	1.51	/	/	1.30[b]
Blaine fineness	390	359	353	400	397	394

(/)Value not determined.
[a] LOI: Loss on ignition.
[b] Correction for oxidation of sulphides has been taken into account.

2.2. Accelerated degradation test

The apparatus for accelerated degradation testing of concrete specimens was used to compare the acid or sulphate resistance of OPC concrete and BFS concrete (Fig. 1a). Cylindrical test specimens (h 70 mm; ø 230 mm) were installed on the machine and before the start of the measurements, the initial distances between the cylinders and the laser sensors were registered with an accuracy of 0.1 mm while the specimens turned at a speed of 24.41 rev/h (5 readings per mm, 4 contour lines per cylinder and 3 cylinders per concrete type). Thereafter, the recipients were filled with 3 l of test liquid, composed of

- 30 g/l acetic and 30 g/l lactic acid, or,
- 29.8 g/l or 3 g/l Na_2SO_4, or,
- 29.8 g/l or 3 g/l $MgSO_4$.

During the experiment, the cylindrical test specimens turned at a speed of 1.04 rev/h. As a consequence, a part of the concrete (radius>90 mm) alternately turned through the solution (1/3 of the rotation time) and the air (2/3 of the rotation time), while another part (radius<90 mm) never came into direct contact with the solution. At the end of each cycle, lasting 7 (for acid attack) or 14 days (for sulphate attack), the cylinders were automatically brushed (so free from user error) to remove all degraded material (Fig. 1b) and the distances were measured by laser sensors (Fig. 1c). Since sulphate attack causes expansion, the change in radius was measured before as well as after brushing. Every week, the simulation liquid was replaced by fresh solution. The details of the degradation testing, including solutions used, cycle duration and differences in measuring procedure for acid and sulphate attack are summarised in Table 3.

The resulting diameter change and surface roughness could be calculated from the initial and subsequent measurements. The convention assumed here was: expansion is positive, reduction is negative. Acid attack and brushing both cause a reduction of the diameter (Δr_t(AB) in Fig. 2). Since sulphate attack and brushing respectively cause an increase and a reduction of the diameter of the test specimens, these two effects were separated. The cumulative increase in radius before brushing at measurement 't' (Σr_t(BB)) was calculated according to formula (1). In this formula, Σr_{t-1}(BB) is the cumulative increase in radius before brushing at the previous measurement ('t − 1'), Δr_t(BB) is the change in radius at measurement 't' before brushing (in comparison to the original radius) and Δr_{t-1}(AB) is the change in radius at measurement 't − 1' after brushing (in comparison to the original radius). The difference between Δr_t(BB) and Δr_{t-1}(AB), is the expansion caused by sulphate attack between the measurements 't − 1' (AB) and 't' (BB). The cumulative radius reduction due to brushing (Σr_t(AB)) was calculated according to formula (2). In this formula, Σr_{t-1}(AB) is the cumulative decrease in radius after brushing at the previous measurement ('t − 1'), Δr_t(AB) is the change in radius at measurement 't' after brushing (in comparison to the original radius) and Δr_t(BB) is the change in radius at measurement 't' before brushing (in comparison to the original radius). The difference between Δr_t(AB) and Δr_t(BB), is the reduction caused by brushing at measurements 't'. A schematic drawing of this principle is shown in Fig. 2.

$$\Sigma r_t(BB) = \Sigma r_{t-1}(BB) + [\Delta r_t(BB) - \Delta r_{t-1}(AB)] \quad (1)$$

$$\Sigma r_t(AB) = \Sigma r_{t-1}(AB) + [\Delta r_t(AB) - \Delta r_t(BB)] \quad (2)$$

The surface roughness of the test specimens is expressed by the R_a-value (in mm), based on the British Standard BS 1134, referring also to ISO/R 468 'Surface roughness'. The R_a-value is defined as the arithmetical average value of the departure y(x) (mm) of the profile above and below the centre line throughout a prescribed sample length L (Eq. (3)). As for concrete cylinders a sample length of 50 mm is advised by De Belie et al. [1], 13 R_a-values are obtained per contour. In Sections 3 and 4, the average of 13 R_a-values per measured contour line, 4 contour lines per cylinder and 3 cylinders per concrete type will be presented as the R_a-value for a certain concrete type.

$$R_a = \frac{1}{L} \cdot \int_0^L |y(x)| dx \quad (3)$$

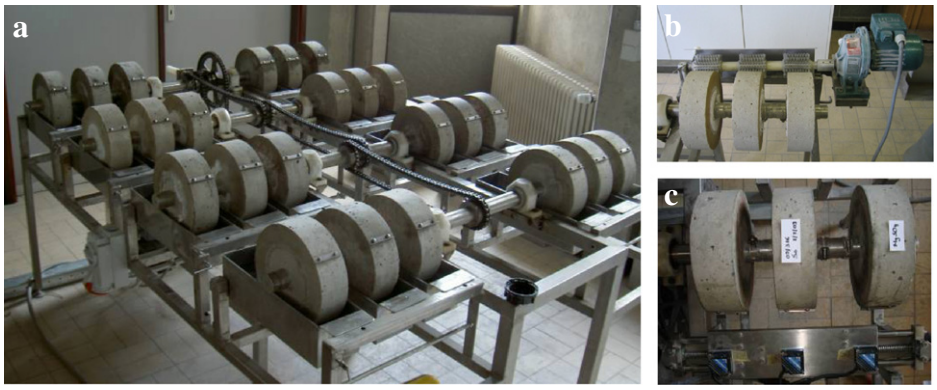

Fig. 1. Apparatus for accelerated degradation testing of concrete specimens.

Table 3
Differences between the measuring procedures applied in case of acid and sulphate attack.

	Acid attack	Sulphate attack
Solution	30 g/l acetic acid + 30 g/l lactic acid	29.8 g/l Na_2SO_4 29.8 g/l $MgSO_4$ 3 g/l Na_2SO_4 3 g/l $MgSO_4$
Replacement of the solution	Every 7 days	Every 7 days
Duration of a cycle	7 days	14 days
Test duration	6 weeks	9 months
Measuring procedure	- Brushing - Measuring	- Measuring - Brushing - Measuring
pH measurement	Daily	Weekly

2.3. Open porosity

The porosity accessible to water was determined by hydrostatic weighing after a vacuum saturation according to the standard NBN B 05-201 paragraph 6.1 (1976). Before the vacuum saturation test, the specimens (h 50 mm; ø 100 mm) were dried until constant mass (mass loss<0.1% in 24 h) in a ventilated oven at (40 ± 5) °C ($m_{d,\ 40\ °C}$) or (105 ± 5) °C ($m_{d,\ 105\ °C}$). Based on the dry (m_d), saturated (m_s) and under water mass (m_l), the open porosity after drying at (40 ± 5) °C and (105 ± 5) °C could be calculated according to formulae (4) and (5).

$$\phi_{40\ °C} = \frac{m_{s,40\,°C} - m_{d,40\,°C}}{m_{s,40\,°C} - m_{l,40\,°C}} \tag{4}$$

$$\phi_{105\ °C} = \frac{m_{s,105\,°C} - m_{d,105\,°C}}{m_{s,105\,°C} - m_{l,105\,°C}} \tag{5}$$

The measuring technique to determine the total open porosity is widely known, although in literature the methods (e.g. [26–31]) slightly differ from each other. In contrast, the method for dividing this porosity into capillary and gel pores is sometimes a matter of discussion. It is not clear whether $\phi_{40\ °C}$ underestimates, overestimates or equals the capillary porosity ϕ_{cap}. Therefore, the porosity (d>0.01 μm) obtained from mercury intrusion porosity (MIP) measurements is compared with $\phi_{40\ °C}$ in Table 4. As can be seen, the correspondence is quite good: $\phi_{(d>0.01\ \mu m)\ MIP}$ is slightly lower than $\phi_{40\ °C}$, except for S85. Remark however that no repetitions were made for the MIP measurements.

It can be concluded that the measuring technique is not completely impeccable and $\phi_{40\ °C}$ does not exactly correspond to ϕ_{cap}. Nevertheless, the characteristics ($\phi_{40\ °C}$ and $\phi_{105\ °C}$) of different specimens, which were equally treated, could be compared with each other and the results are presented in Section 3.

2.4. Thermogravimetric analyses

Because lactic and acetic acids combine primarily with CH, the CH content in cement paste is very important and can be determined by means of thermogravimetric (TG) analyses. To monitor the evolution as a function of time, the hydration of the binding agents was stopped at different ages, ranging from 18 h up to 1 year, by soaking crushed cement paste in methanol for 7 days and subsequently drying it in a desiccator. The obtained samples were then exposed under an inert atmosphere to increasing temperatures, ranging from 20 °C till 850 °C at a rate of 10 °C/min.

CH decomposes into CaO and H_2O between 410 and 480 °C. Taking into account the molecular weights of calcium hydroxide (MW_{CH}) and water (MW_{H2O}), the weight loss in percent during CH dehydration (WL_{CH}) can be converted to the amount of CH [32] (term 1 of formula (6)). Moreover, the weight loss recorded at a temperature of ~670 °C corresponds with the decomposition of $CaCO_3$ into CaO and CO_2 (WL_{CaCO3}). Since the $CaCO_3$ originated on the one hand from the original cement and slag ($WL_{original\ CO2}$ = ~0.7%, ~0.5% and ~0.35% respectively for S0(CP), S50(CP) and S85(CP) — values based on the CO_2 content (Table 2) of the raw materials used for TG measurements (OPC(I) and BFS(I)/OPC(II) and BFS (II))) but on the other hand from the chemical carbonation reaction between CH and CO_2 [33], the original CH content, irrespective of carbonation of the samples, can be calculated according to formula (6). However, it must be remarked that the CH value can be slightly overestimated since part of the $CaCO_3$ also originates from the carbonation of C–S–H [34].

$$CH(\%) = WL_{CH}(\%) \cdot \frac{MW_{CH}}{MW_{H_2O}} + \left(WL_{CaCO_3}(\%) - WL_{originalCO_2}(\%)\right) \cdot \frac{MW_{CH}}{MW_{CO_2}} \tag{6}$$

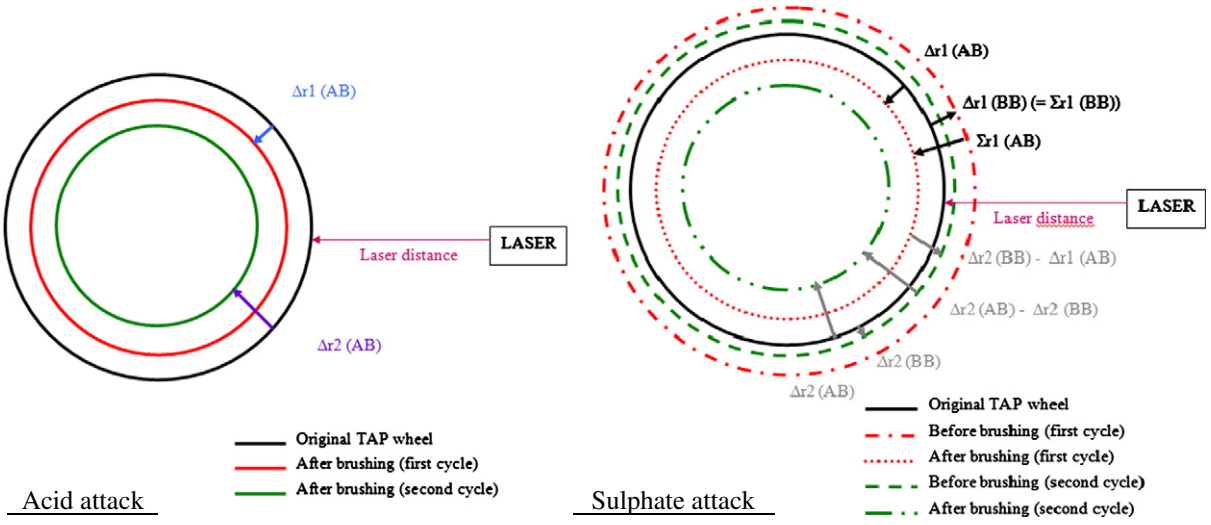

Fig. 2. Schematic drawing of the degradation processes of cylinders exposed to a lactic–acetic acid solution after brushing (AB) (left) or to a sulphate solution before (BB) and after brushing (AB) (right).

Table 4
Comparison between the porosity (d>0.01 μm) obtained by mercury intrusion porosimetry (MIP) and $\varphi_{40\ °C}$ (porosity accessible to water after drying at 40 °C until constant mass) (%).

	S0	S50	S70	S85
$\varphi_{(d>0.01\ \mu m)}$ MIP (5 months)	8.8	8.1	8.7	13.3
$\varphi_{40\ °C}$ (6 months)	9.4[a]	9.1[a]	9.2	9.6

[a] Not measured: interpolation between $\varphi_{40\ °C}$ at 3 M and $\varphi_{40\ °C}$ at 12 M.

The weight losses WL_{CH} and WL_{CaCO3} were corrected for the concurrent dehydration of all other hydrates, according to the method described by Baert [35].

3. Acid resistance

Fig. 3 shows concrete cylinders (OPC(II), BFS(II)) before and after 6 acid attack cycles for the 4 concrete types (S0, S50, S70 and S85) tested after an initial curing time of 1 month. Obviously, the OPC concrete deteriorated the most. When the specimens were tested after 6 months of curing, a similar trend could be observed after a few cycles. The average accumulated reduction in radius (after every cycle) of the concrete cylinders (initial curing time: 1 or 6 months) is presented in Fig. 4. As can be clearly seen, the acid resistance of OPC concrete is the lowest and the attack depth of BFS concrete is less than 0.5 mm. Since the differences between the concrete mixes with different amounts of slag are rather small, a univariate, multi-way ANOVA test was executed. In advance, the homogeneity of the variances was checked with a Levene's test (two tails and level of significance = 0.01). Since the variances were not homogeneous ($P<0.001$) and the interaction between the factors 'cycle number, curing time and slag content' was significant ($P<0.001$), a univariate one-way ANOVA and Dunnett's T3 Post Hoc test was performed, considering 48 different groups. The results, tabulated in Table 5, indicate that the acid resistance of S0 is always significantly ($P<0.05$) lower than that of S50, S70 and S85. Although it looked as if increasing the BFS content above 50% yields a limited improvement in acid resistance, the differences between the BFS concrete mixes are not significant ($P>0.05$). Remark that an increase of the BFS content above 50% involves a considerable reduction in 28 day compressive strength (see Table 1). Moreover, only S0 performs significantly better after a curing time of 6 months (in comparison to 1 month) during the first attack cycles. After 5 cycles, the significant differences also disappear for S0.

Besides the degradation depth, the surface roughness was also calculated. Before degradation by the organic acids, the roughness of the specimens is about the same for all concrete types and amounts to ~0.064 mm. After merely 2 cycles, the surface roughness of OPC concrete can be distinguished from that of BFS concrete. Finally, after six cycles a R_a-value of 1.1–1.2 mm is reached for OPC concrete, whereas concrete in which 85% of the cement was replaced by BFS has a roughness value of ~0.2 mm (Fig. 5).

A highly aggressive test liquid, composed of 30 g/l acetic acid (0.50 mol/l) and 30 g/l lactic acid (0.33 mol/l), was used in these experiments. These acid concentrations correspond quite well with the highest concentrations measured in samples taken from floors in pig houses. However, the pH of the simulation liquid was 2, while the pH in real conditions varies between 3.8 and 4.5. This difference is due to the absence of buffering feed ingredients in the simulation liquid [5,7,9]. Lactic and acetic acids are both weak acids. According to their pK_a value (3.86 for lactic acid and 4.75 for acetic acid), lactic acid will dissociate first and react with CH, the most vulnerable phase in concrete towards acid attack. Depending on the type of concrete mixture and number of acid test cycles applied, the pH of the bulk solution was observed to increase from 2 to 3.5–5.5. For an increase up to pH 3.5, this indicates that about 30% (0.100 M) and 5% (0.025 M) of lactic and acetic acids, respectively, were neutralised as a result of leaching of hydroxyl ions from the concrete matrix. For an increase up to pH 5.5, this indicates that about 98% (0.326 M) and 85% (0.425 M) of lactic and acetic acids, respectively, were

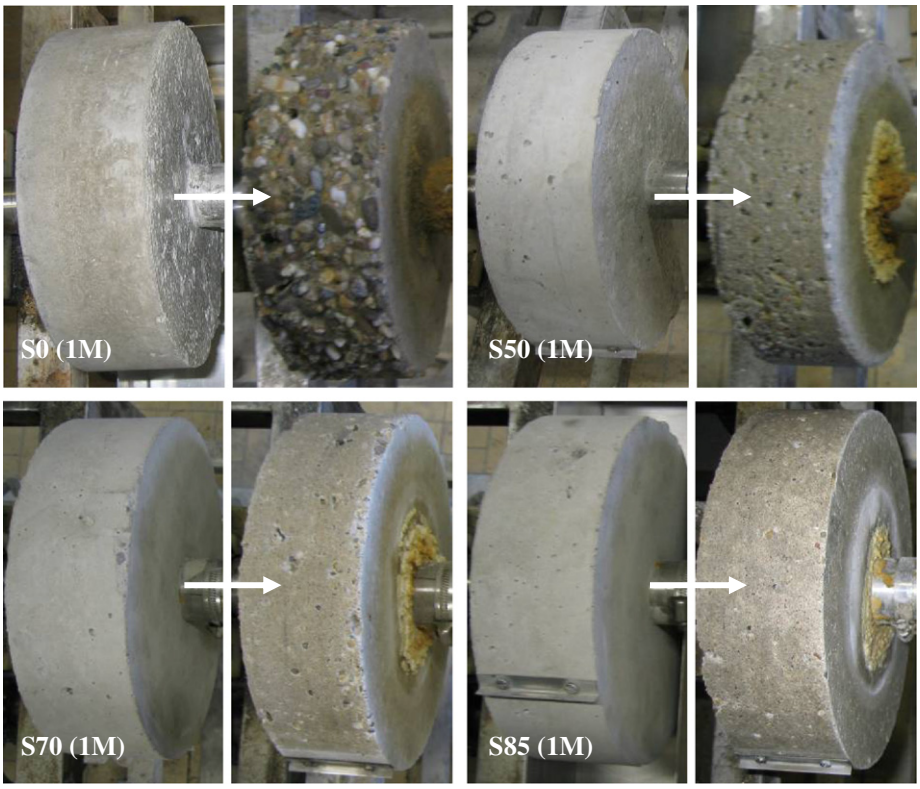

Fig. 3. Image of the test specimens before and after the acid attack.

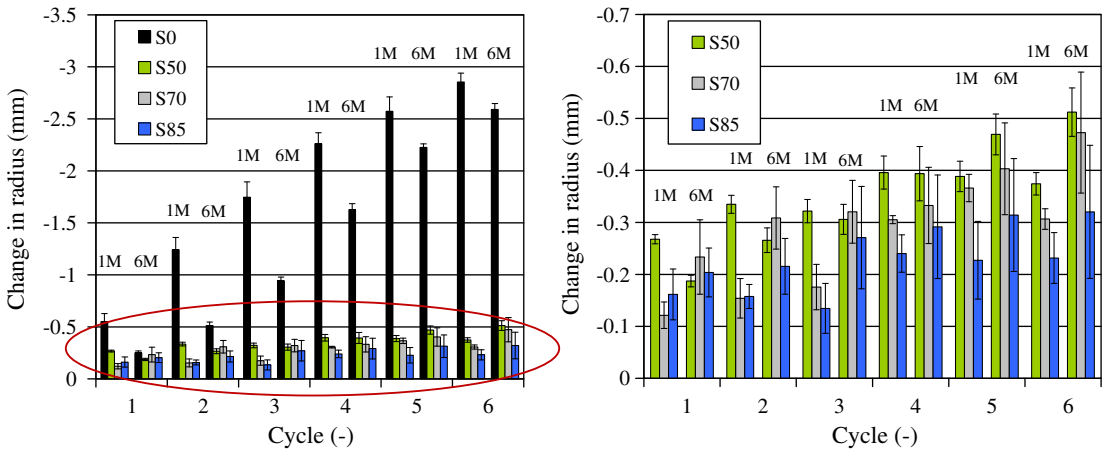

Fig. 4. Reduction in radius of the cylindrical test specimens exposed to lactic–acetic acid solutions and tested at the age of 1 and 6 months. The figure at the right is an enlargement of the encircled area in the left hand figure.

neutralised. As can be seen in Fig. 6, OPC concrete has the highest neutralising capacity which is however reduced during the subsequent attack cycles. This indicates that the decalcification of CH, $CaCO_3$ and C–S–H is reduced (i) during subsequent cycles (since Ca^{2+} has already been leached out during preceding cycles and the decalcification front is thus located deeper) and (ii) for concrete containing increasing amounts of BFS. Based on the observed pH increase, it can thus be concluded that BFS concrete has a higher chemical resistance towards acid attack than OPC concrete. When the replacement percentage is increased from 50% up to 85% merely a slight increase in acid resistance could be recorded. These conclusions correspond with the surface degradation depth measurements, as shown above.

The penetration of acids depends on the open porosity of the concrete mix. As can be seen in Fig. 7, the mean values of $\phi_{40\,°C}$ (and $\phi_{105\,°C}$) generally decrease slightly with time while ($\phi_{105\,°C} - \phi_{40\,°C}$) increases. Moreover, the ratio of $\phi_{40\,°C}$-to-$\phi_{105\,°C}$ decreases with increasing curing time for each of the mixtures, indicating a refinement of the pore structure (0.75 (S0); 0.68 (S50); 0.62 (S70) or 0.65 (S85) (curing time: 1 month) → 0.65 (S0); 0.61 (S50); 0.59 (S70) and 0.60 (S85) (curing time: 6 months)). Nevertheless, a statistical analysis (One-way ANOVA and Scheffé Post Hoc test) only detects a significant difference between $\phi_{40\,°C}$ of S0 after curing for 1 and 6 months. Since $\phi_{40\,°C}$ decreases, the penetration of acids into concrete is hindered which leads to a better acid resistance, as described above. In comparison to OPC concrete, the pore structure of BFS concrete is finer: the ratio of $\phi_{40\,°C}$-to-$\phi_{105\,°C}$ is smaller. However, significant differences were only detected for ($\phi_{105\,°C}$–$\phi_{40\,°C}$) between S0 and S70, S85 (curing time: 1 month). After a curing time of 6 months, $\phi_{105\,°C}$ of S0 (smaller total porosity) differs significantly from S70 and S85, and there is also a significant difference between S50 (smaller total porosity) and S85.

Penetration of acids is a function of porosity and tortuosity. However, since the differences between the open porosity (porosity accessible to water) of OPC and BFS mixes are not that pronounced, this cannot be the main influencing parameter to explain the results obtained here. The different acid resistances must also be caused by the nature of the hydration products. Since the deterioration mechanism starts with the production of soluble calcium salts from the reaction of lactic–acetic acid and CH, the CH-content of the hydrated concrete mix is of major importance [4,5,7]. In Table 6, the CH-contents (without (CH*) and with (CH) correction for carbonation) for the cement pastes S0(CP), S50(CP) and S85(CP) after different curing times are given. As can be seen in Fig. 8, the CH-content (expressed in g per 100 g binder) in pastes decreases with increasing BFS content at very early age. However, the decrease is not proportional to the cement replacement percentage. For the cement pastes S30(CP) and S50(CP) and for most of the specimens S85(CP), the CH-content, expressed in g per 100 g cement, is higher than in pure cement paste, indicating an enhancement of the cement hydration

Table 5
Significant differences in reduction in radius between the concrete mixes (One Way ANOVA and Dunnett's T3 Post Hoc test) (S = significant difference (P<0.05); NS = no significant difference (P>0.05)).

Compared compositions	Cycle 1	Cycle 2	Cycle 3	Cycle 4	Cycle 5	Cycle 6
1 month						
S0–S50, S70, S85	S	S	S	S	S	S
S50–S70	S	NS	NS	NS	NS	NS
S50–S85	NS	S	NS	NS	NS	NS
S70–S85	NS	NS	NS	NS	NS	NS
6 months						
S0–S50, S70, S85	NS	S	S	S	S	S
S50–S70	NS	NS	NS	NS	NS	NS
S50–S85	NS	NS	NS	NS	NS	NS
S70–S85	NS	NS	NS	NS	NS	NS
1 month–6 months						
S0	S	S	S	S	NS	NS
S50	NS	NS	NS	NS	NS	NS
S70	NS	NS	NS	NS	NS	NS
S85	NS	NS	NS	NS	NS	NS

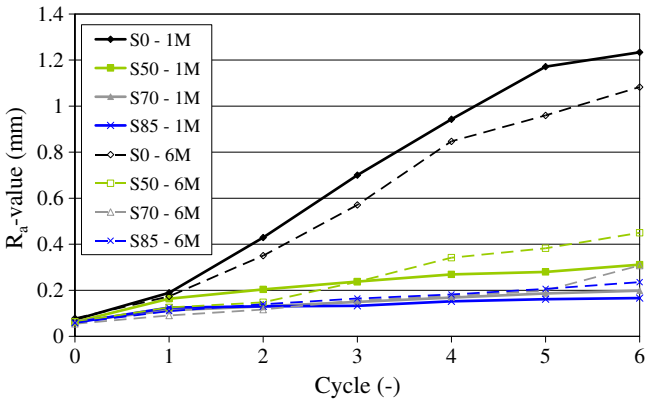

Fig. 5. R_a-value of the concrete specimens with 0%, 50%, 70% and 85% of the cement replaced by BFS after every acid attack cycle at an age of 1 and 6 months.

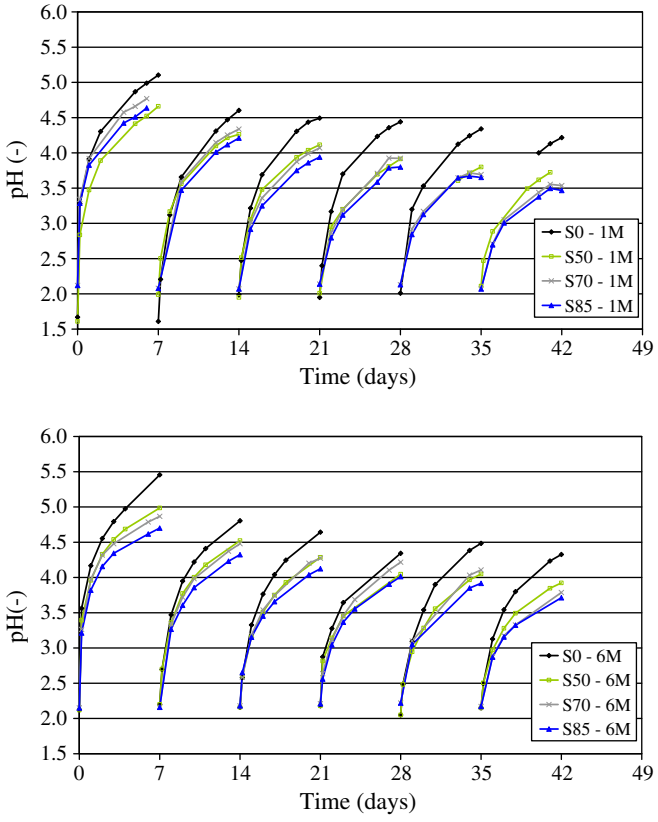

Fig. 6. pH of the simulation liquid during the test.

in the presence of BFS. According to Escalante-Garcia and Sharp [36], who also recorded an enhanced hydration of the four anhydrous phases when slag is added, this could be due to heterogeneous nucleation, the dilution effect, the fixation of Ca^{2+} and SO_4^{2-} ions which accelerates the hydration of interstitial phases and the consumption of CH during the slag hydration. According to Stark et al. [37], the accelerating effect due to heterogeneous nucleation can only be attained when the specific surface area of BFS is high enough. Since the fineness of the cement and slag, used in the current research, are roughly equal, the contribution of heterogeneous nucleation towards the acceleration of the OPC reaction is probably limited. However, isothermal calorimetric tests performed on cement pastes with different w/c ratios (w/c≥0.5) and pastes containing slag (w/b=0.5 and s/b=0.3, 0.5 and 0.85), show that the presence of slag and not the increase in w/c ratio (>0.5) is responsible for the acceleration effect [38]. Furthermore, since the slag reaction only starts when the correct

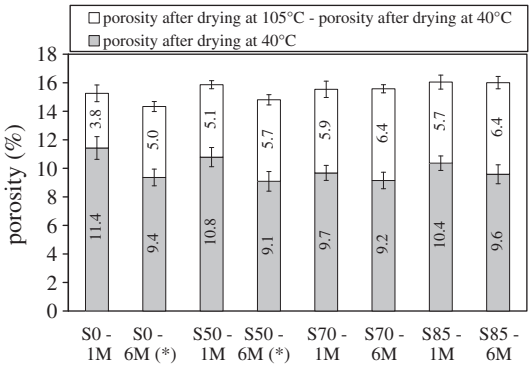

Fig. 7. $\phi_{40\ °C}$, $\phi_{105\ °C}$ and $\phi_{105\ °C} - \phi_{40\ °C}$ of the four mixes with 0%, 50%, 70% and 85% of the cement replaced by BFS (OPC (II), BFS (II)) at 1 and 6 months. (*): values obtained by linear regression of the porosity measurements at 3 and 9 months.

Table 6
CH content (expressed in g/100 g binder) of cement pastes S0(CP), S50(CP) and S85(CP) after different curing times. 'CH*' is the CH content determined according to term 1 of formula (6) (no correction for carbonation), 'CH' is the CH content determined according to formula (6) (with correction for carbonation). The bold results indicate that $CaCO_3$, due to carbonation, was present.

Curing time	S0(CP)		S50(CP)		S85(CP)	
	CH*	CH	CH*	CH	CH*	CH
18 h	6.5	6.5	4.0	4.0	0.6	**0.9**
21 h	7.8	7.8	4.3	4.3	0.8	0.9
24 h	9.2	9.2	4.5	**5.1**	1.0	**2.1**
30 h	10.6	10.6	5.4	5.4	1.2	**1.9**
4 days	15.8 [a]	**17.2** [a]	7.0	**7.8**	0.6	**3.2**
7 days	15.9	16.0	6.6	**8.2**	0.9 [b]	**2.0** [b]
14 days	17.3	**17.8**	6.6	**7.7**	0.6	**2.1**
28 days	19.0	19.0	6.4	**8.6**	1.1 [c]	**1.3** [c]
56 days	18.9	18.9	7.6	7.6	1.1	**3.1**
91 days	18.0	18.0	6.6	6.6	0.9	0.9
182 days	18.0	**18.4**	7.9	7.9	/	/
280 days	16.3	16.3	6.2	6.2	0.7	**4.5**
364 days	18.4	18.5	7.3	7.3	0.4	**2.5**

[a] 5 days instead of 4 days.
[b] 8 days instead of 7 days.
[c] 30 days instead of 28 days.

alkalinity is reached [39], what occurs generally during the second day (at hydration temperatures of 20 °C) [40], the consumption of CH during the BFS hydration cannot be the main cause of the enhanced cement hydration during the first day. However, from the second day onwards, the CH-content susceptible to acid attack, decreases slightly more than proportional with the replacement

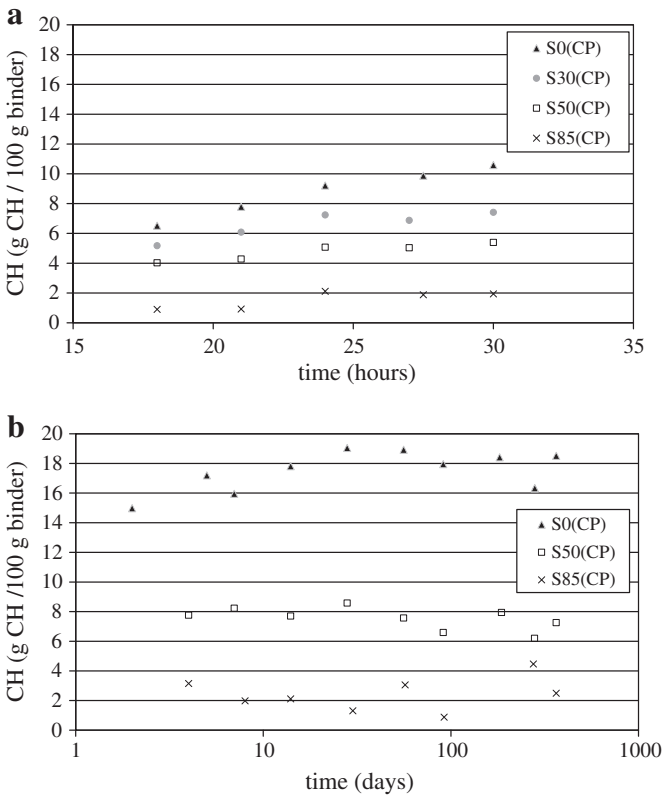

Fig. 8. (a) CH content of S0(CP), S30(CP), S50(CP) and S85(CP) (OPC (II), BFS (II)) after 18 to 30 h of hydration. (b) CH content of S0(CP), S50(CP) and S85(CP) (OPC (I), BFS (I)) after 2 to 364 days of hydration.

percentage (Fig. 8 (b)), indicating a limited consumption of CH, liberated during the cement hydration, when slag hydrates. This effect is shown more clearly in Fig. 9.

After 1 month, the values of CH in S0(CP) and S50(CP) fluctuate between 17 and 19% respectively 6 and 8%. These fluctuations around a mean value are, based on our test results, within experimental error (~2%). Moreover, the test specimens are very small (and thus very sensitive to slight changes in composition) and Fig. 8 was plotted based on only one test result at each age. Concerning S85(CP), the mass losses during CH decomposition are very small (leading to a CH content of 0–1 g per 100 g binder — see Table 6) and some test specimens are carbonated, which results in a reduced accuracy for the determination of the CH-content. Moreover, as mentioned in Section 2.4, the CH value can be slightly overestimated (especially for BFS mixes) since part of the $CaCO_3$ also originates from the carbonation of C–S–H.

Thus, BFS concrete has a low CH content and in comparison to OPC concrete this content is reduced more than proportional to the cement replacement percentage. Besides the reaction with CH, which decomposes at a pH below 12, also calciumsulphoaluminates decompose (pH<11) and C–S–H decalcifies when the pH drops [41]. Since Ca dissolves more easily than Si and the C/S ratio of C–S–H in OPC concrete is higher than in BFS concrete, OPC concrete is more vulnerable towards acid attack (see Figs. 3, 4 and 5). Before brushing it could be clearly observed that the attacked layer is more porous and has almost no mechanical strength. Therefore, this layer could be easily removed by brushing. In BFS concrete, the CH-content is lower (see Fig. 8), the C/S ratio in the hydration products is lower [42] and the dissolution of Ca [10] from C–S–(A—)H leads to the formation of a (alumino)silicate gel. Since this semi-permeable layer protects the specimen from further degradation [41], the acid resistance of BFS concrete is higher than that of OPC concrete. According to Bertron et al. [8] a better acid resistance is only obtained if the CaO content is limited as well as the amount of SiO_2 is increased (a decrease of the C/S ratio is not sufficient). Moreover, the presence of secondary elements such as iron and aluminium is favourable. The values in Table 2 clearly show that BFS (as used in the current research) has a lower content of CaO and a higher content of SiO_2 than OPC and therefore satisfies the requirements to reduce the degradation due to acid attack. Furthermore, in comparison to OPC, the content of Al_2O_3 is higher but the content of Fe_2O_3 is lower in BFS.

In Fig. 10, the test results of the current research are compared with those of earlier research performed by De Belie [2]. The concrete mixes used in the work of De Belie had a cement content of 375 kg/m^3 and a w/c ratio of 0.39. Only the test results of concrete containing OPC concrete (CEM I 42.5 R (comparable with the currently used CEM I 52.5 N)) and concrete made with slag blended cement (CEM III/A 42.5 → s/b = 0.36–0.65) are presented. The test conditions (acid concentration, duration, measuring procedure) were the same in both studies and the results can thus be compared. As can be seen in Fig. 10, the acid resistance (degradation depth as well as surface roughness) of reference concrete mixes increases with decreasing w/c ratios (0.5 ↔ 0.39). Moreover, it seems that BFS, whether added as a separate component or as a component in blast-furnace slag cement, improves the acid resistance of concrete.

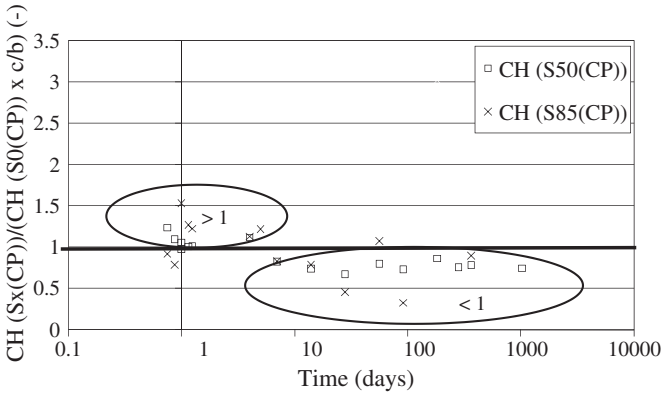

Fig. 9. Ratio of the CH-content of Sx(CP) (containing 50 or 85% slag) to that of S0 (CP) × c/b in function of time.

4. Sulphate resistance

4.1. Sodium sulphate

The concrete specimens, made with (OPC(III), BFS(III)), turned alternately through the sulphate solution and the air. Alternating wetting and drying was supposed to accelerate the degradation mechanism because of the enhanced accumulation of sulphate ions in the concrete. An image of the test specimens before and after 37 weeks of cyclical exposure to a 29.8 g/l Na_2SO_4 solution is shown in Fig. 11. As can be seen, the circumferential surfaces of S85 are most degraded while those of S0 remained almost intact. The change in radius over this time period was monitored and the results (mean values of 3 concrete specimens) are presented in Fig. 12. As mentioned in Section 2.2, the effects of sulphate attack and brushing were separated and the actual change in radius is obtained by a combination of both. First of all, it must be remarked that these actual changes (in comparison to the original radii) are very small. After each cycle, the changes before and after brushing (relative to the original radius) are always less than 0.3 mm and in most of the cases even less than 0.1 mm. Since the accuracy of the laser sensors is merely ~0.1 mm, the differences are thus seldom significant. As a consequence, small errors accumulate when the cumulative changes in radii due to sulphate attack and brushing are considered. Moreover, this explains why positive values (corresponding to expansion) could be obtained for the changes in radii due to brushing. In principle, brushing only removes loose material and can thus only correspond with a reduction of the radius. Furthermore, the three specimens of each measurement series do not all evolve the same. The standard deviation on the mean values is therefore (in some cases) rather high. To maintain the overview, no error bars were indicated in Fig. 12, but an example is given in Fig. 13. In spite of these uncertainties, the values in Fig. 12 clearly indicate that replacement of cement by high amounts of slag (85%) is more detrimental. The cumulative changes in radii due to sulphate attack and brushing are much higher than those obtained for OPC concrete. Moreover, these findings are also confirmed by visual inspection (Fig. 11) and roughness measurements (Fig. 14). While the evolution of the R_a-values is quite similar for S0, S50 [a] and S50 [b], a stronger increase was recorded for S85. This statement was also confirmed by statistical analysis (one way ANOVA and Dunnet's T3 Post Hoc test). For S0, S50 [a], S50 [b] and S85, the R_a-values after 37 weeks were respectively 1.45, 1.46, 1.64 and 2.43 times higher than the initial values. Concerning the effect of 50% cement replacement by slag, it is difficult to draw conclusions: the evolution of the surface roughness as well as the changes in radii indicates that the performance of S50 [b] is worse than that of S0 while the damage caused by a 3 g/l Na_2SO_4 solution on S50 [b] is slightly higher than that of a 29.8 g/l Na_2SO_4 solution on S50 [a]. We suppose that either the limited resolution of the measurements is the cause or the reaction mechanism changes since the concentration differs. From literature review ([43,44] cited by [45]), it seemed that in Na_2SO_4 solutions ettringite formation is favoured at low concentrations, while gypsum is preferentially formed at high concentrations.

The results above all consider the degradation of the circumferential surfaces of the concrete cylinders which were cyclically submerged in the sulphate solution. However, visual observation of the test specimens (Fig. 11) indicated that the part which never came into direct contact with the sulphate solution suffered most from sulphate deterioration. Crystals ('soft' and white) were formed on the surface and the concrete underneath the crystals was more degraded than the circumferential

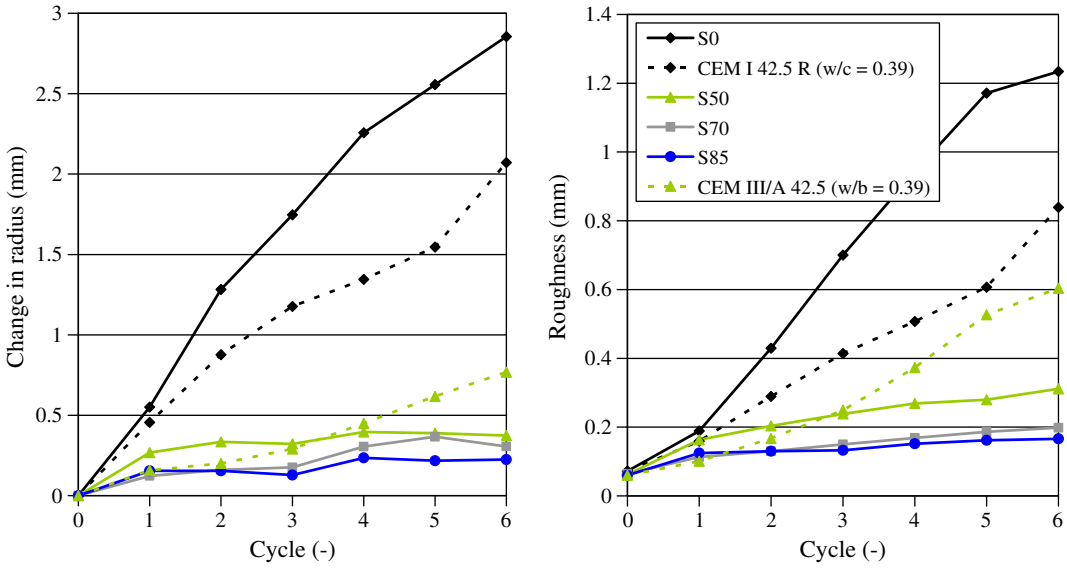

Fig. 10. Cumulative change in radius and surface roughness of test specimens exposed to lactic and acetic acid solutions (test age = 1 month). Comparison between the test results of the current research (S0, S50, S70 and S85) and those of earlier research performed by De Belie [2].

surfaces (Figs. 15 and 16). The higher the cement replacement level, the more crystals were formed and the more degraded the specimens were.

For the S85 specimens, the surface layer had completely disappeared and the aggregates were clearly visible. The outermost concrete layers also crumbled easily. Samples for XRD measurements were taken by means of a thin blade from the outermost concrete layers and from the crystals formed on the surface of the specimens. XRD analyses were performed immediately and showed that thenardite (Na_2SO_4) was formed on the surface, while thenardite and calcite could be found in the outermost concrete layers. Calcite, which is an important factor to build up crystallisation pressure (see Section 1) and consequently damage [12,46,47], is thus available in the S85 specimens. This is not surprising since these BFS concrete mixes are very susceptible to carbonation [38] (this can also be concluded from the values in Table 6). In Fig. 16 it can be seen how the specimens were split into three parts after the tests. On the inner parts, phenolphthalein solution was sprayed in order to estimate the carbonation depth (Table 7). The trowelled surfaces which were most degraded also showed a slightly higher carbonation depth.

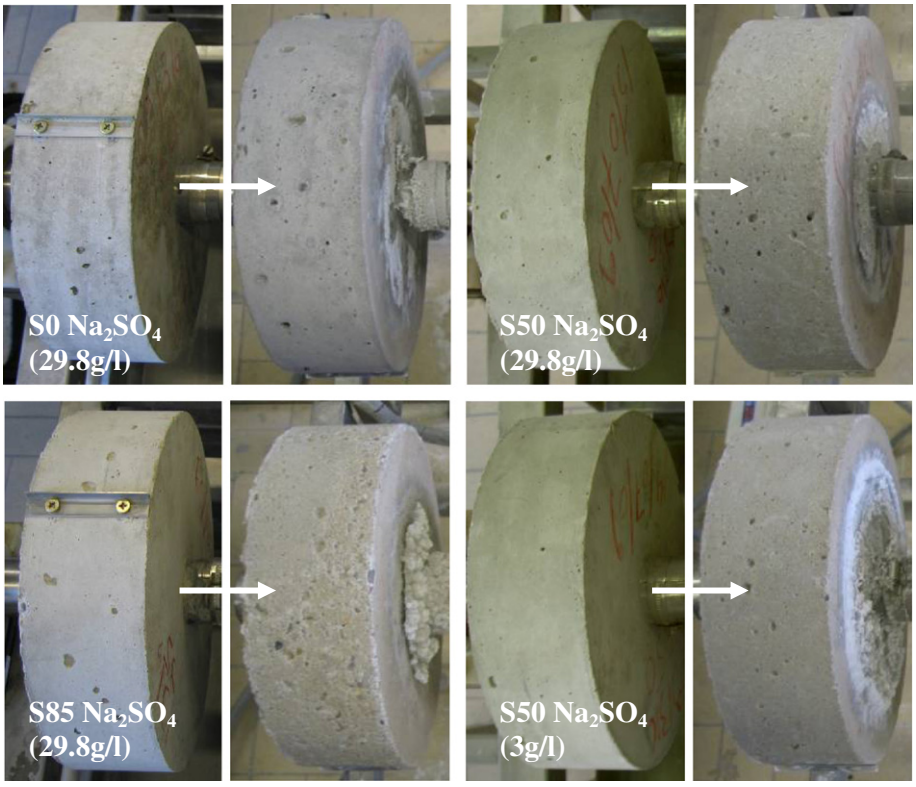

Fig. 11. Image of concrete test specimens before and after 37 weeks of cyclical exposure to Na_2SO_4 solutions.

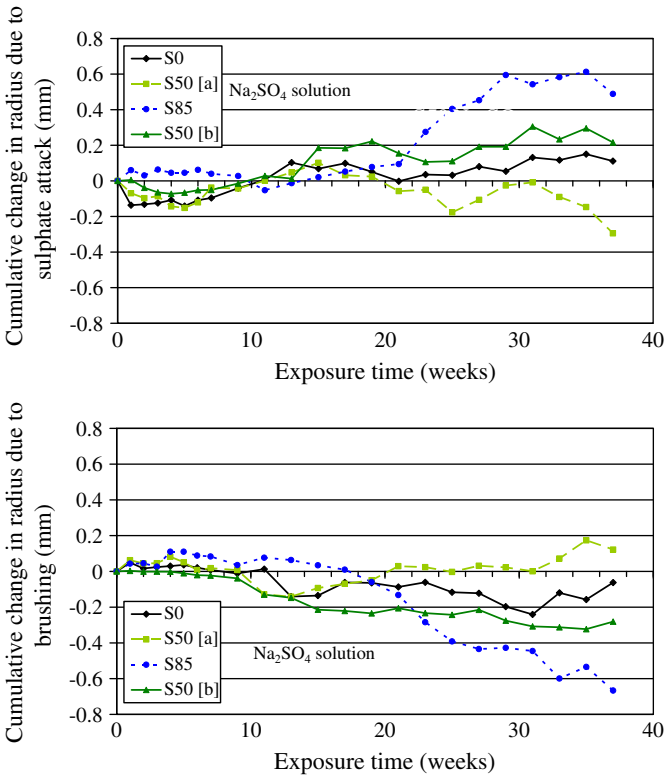

Fig. 12. Cumulative change in radius due to sulphate attack (above) and brushing (below) for test specimens cyclically exposed to a 29.8 g/l Na_2SO_4 solution (S0, S50 [a] and S85) or a 3 g/l Na_2SO_4 solution (S50 [b]).

Although S50 [a] specimens also suffered from crystallisation, the degradation of the concrete was less than that of S85. Both the S50 [a] and S50 [b] specimens suffered from carbonation (Table 7), but the damage caused by the less concentrated sulphate solutions to the S50 [b] specimens was much lower.

The resistance against sulphate attack was the highest for OPC concrete. Less thenardite crystals were formed on the surface and the concrete below the crystals remained rather intact (although thenardite and calcite were also found in the outermost layer).

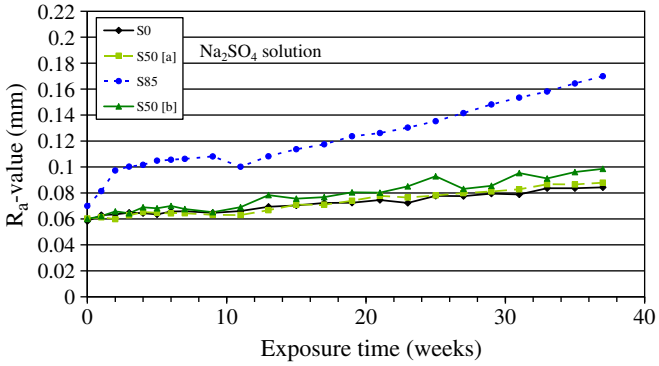

Fig. 14. Evolution of the surface roughness of concrete specimens with different amounts of BFS. The concentration of the Na_2SO_4 solutions was 29.8 g/l for S0, S50 [a] and S85 and 3 g/l for S50 [b].

The fact that OPC concrete performs better than BFS concrete in case of partial submersion contrasts sharply with the situation of complete submersion of mortars: Tests (based on ASTM C 1012-04, the Wittekindt procedure and the SVA-method [48,49]) performed by Gruyaert [38] on completely submerged mortar mixtures containing different amounts of BFS (of the same chemical composition) showed that BFS mortar (s/b = 0.5 or 0.85) performed significantly better than OPC mortar. The different behaviour is caused by the difference in attack mechanism (physical versus chemical). The bad performance of concrete containing high amounts of BFS (S85) in case of partial submersion is attributed to the buildup of salt crystallisation pressure (in the parts which were not submerged).

The testing apparatus for accelerated degradation tests was originally developed to accelerate degradation processes by alternating wetting and drying and brushing. However, application of the apparatus in that way for sodium sulphate attack does not allow to measure the degradation in the zone (side faces) which is most attacked. Therefore, it is advised to use the equipment in a different way to study sodium sulphate attack. In future research, stationary concrete cylinders can be partially

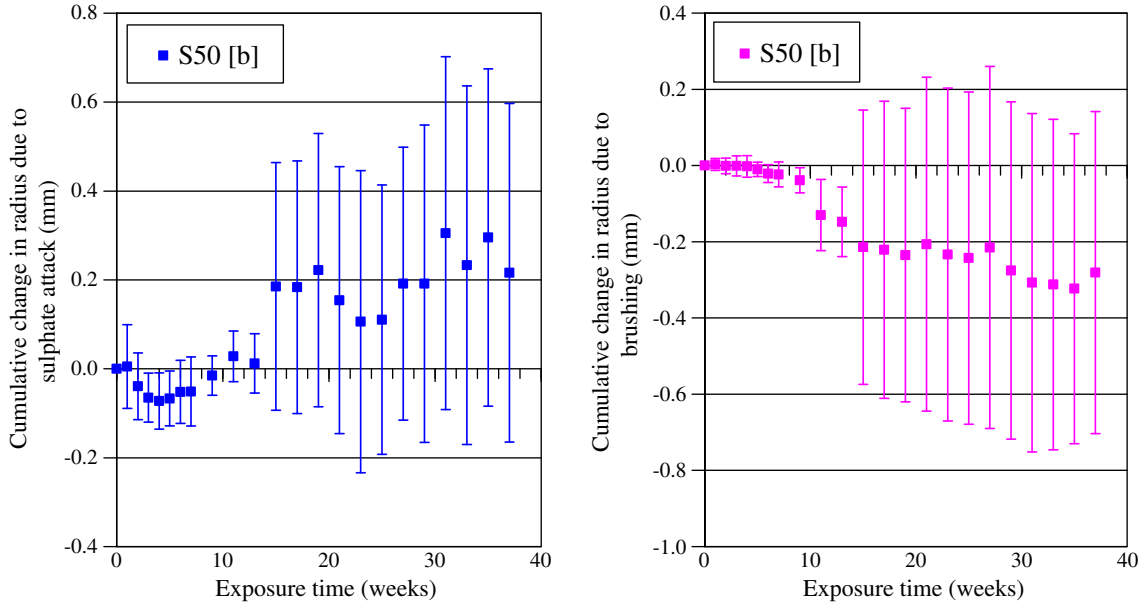

Fig. 13. Average expansion and reduction in radius of the test specimens S50 [b] (n = 3) due to sulphate attack (left graph) respectively brushing (right graph), with indication of the standard deviation.

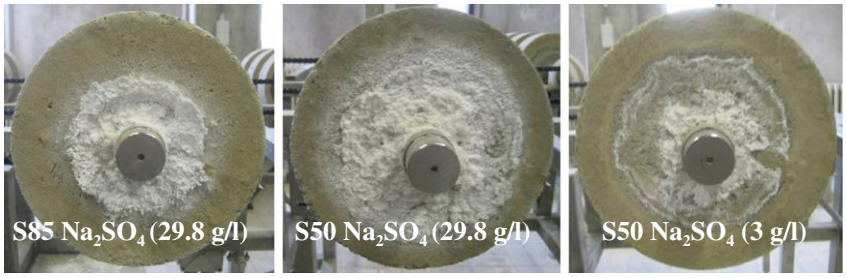

Fig. 15. Crystallisation on the concrete specimens (exposure time: 37 weeks).

submerged in the solutions. Just above the liquid level, crystals will then be formed on the surface and the concrete below the crystals will degrade. Brushing of the test specimens can then remove the 'soft' and 'crumbly' concrete underneath the crystals and accelerate the degradation process. Measurements of the change in radius and surface roughness can give a quantitative indication of the sulphate resistance of partially submerged concrete specimens.

4.2. Magnesium sulphate

An image of the concrete cylinders (OPC(III), BFS(III)) before and after 37 weeks of cyclical exposure to $MgSO_4$ solutions is shown in Fig. 17. Again, concrete containing 85% BFS is most deteriorated while OPC concrete performed well. Moreover, the degradation caused by $MgSO_4$ seems to be slightly higher than that caused by Na_2SO_4.

In Fig. 18, the expansions and reductions in radius due to sulphate attack and brushing are presented (mean values of 3 concrete cylinders). No results could be shown for S50 [b] because the laser sensors could not be adjusted well on the metal reference plates. As a consequence, different measurements could not be compared and the cumulative change in radius could not be calculated. Contrarily, the surface roughness, which was determined based on each of the individual profiles, could be determined. The same remarks as mentioned above concerning the accuracy of measurements are valid.

As can be seen in Fig. 18, a reduction of the radius is recorded during the first attack cycles. Thereafter, sulphate attack causes a continuous expansion of the concrete cylinders S50 [a] and S85. On the other hand, brushing leads to a continuous reduction of the radius for all concrete mixes. After 37 weeks, S85 shows the highest expansion, but also the highest reduction due to brushing. The resulting effect is a reduction of −0.27 mm compared to the original radius. For S0 and S50 [a], these values amount to −0.34 and −0.19 mm. The high value of S0 does not mean however that these specimens are most degraded: sulphate attack causes a reduction in radius (−0.12 mm), which is very small in comparison to the accuracy of the measurements and this negative value increases the reduction due to brushing (−0.22 mm). If the surface roughness values are also considered (Fig. 19), the overall conclusion is that S0 and S50 [a] perform quite similar, while the performance of S85 is worse. After 37 weeks, the R_a-value is increased by a factor 1.69, 1.71, 1.31 and 3.20 for S0, S50 [a], S50 [b] and S85, respectively. The surface roughness of S85 at the end of the experiment was significantly higher than that of S0, S50 [a] and S50 [b]. S50 [a] and S50 [b] also differed significantly from each other, but both of them did not differ significantly from S0. All these findings correspond quite well with the visual observation (Fig. 17).

The parts of the test specimens which never came into direct contact with the solutions are covered with a crystallisation product (Fig. 20). In comparison to the crystals formed in case of Na_2SO_4 attack, the deposit is hard and has a light grey colour. Moreover, the concrete beneath is less deteriorated, but it was difficult to remove the crystals. As the sulphate concentration decreases, the crystallisation and damage is reduced. XRD analysis of the crystals revealed that epsomite is formed ($MgSO_4.7H_2O$), while calcite was detected in the outermost concrete layers. Carbonation of the concrete specimens was confirmed by spraying phenolphthalein solution on the freshly broken concrete (Table 7).

5. Conclusion

5.1. Acid attack

Measurements of the degradation depth, surface roughness and pH increase of the acid solutions all show the same trend: BFS concrete, exposed to a lactic–acetic acid solution (pH~2), performs significantly better than OPC concrete. The concrete's acid resistance does not improve considerably if the cement replacement percentage is increased from 50% to 85% (remember however that the compressive strength of S50 equals that of S0, while S85 has a considerably lower mechanical performance). Since lactic and acetic acids leach out Ca-ions, the better performance of BFS concrete was mainly due to the lower CaO content and the higher SiO_2 content of BFS. Because of the higher CH content and higher C/S ratio in the cement hydration products, OPC concrete is more vulnerable towards acid attack: the attacked layer is porous, has almost no mechanical strength and can be easily removed by brushing. In BFS concrete, the CH content is strongly reduced, the C/S ratio in the hydration products is lower and decalcification leads to the formation of a silica(alumino)gel. From literature review it seemed that this layer hinders the further ingress of acids and contributes towards the better acid resistance of BFS concrete.

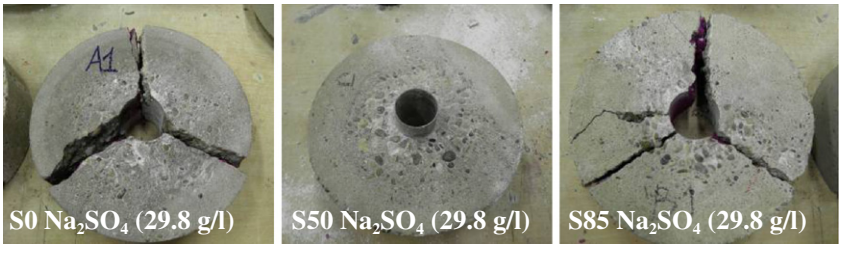

Fig. 16. Degradation of the concrete specimens underneath the crystals (trowelled surfaces) (exposure time: 37 weeks).

Table 7
Mean carbonation depth (mm) of the side surfaces of the test cylinders partly submerged in sodium/magnesium sulphate solutions (datum point = original side surface).

Carbonation depth (mm)	S0	S50 [a]	S50 [b]	S85
Na_2SO_4	1.3	2.7	3.6	2.5
$MgSO_4$	1.5	1.6	2.8	2.8

5.2. Sulphate attack — cyclically and partially submerged concrete

The circumferential surfaces of the cylinders, which alternately turned through the sulphate solutions and the air, were most degraded for concrete containing high amounts of BFS. The performance of S0 and S50 was almost similar. However, in comparison to the side surfaces which never came into contact with the solution, this deterioration was negligible. Crystals were formed on these side surfaces and the concrete below these crystals was degraded, especially for the mixtures containing high amounts of BFS and for the trowelled surfaces. From literature review, it seemed that crystallisation pressure can be built up in carbonated cementitious materials (carbonation was demonstrated here by XRD analysis and spraying phenolphthalein solution) and damage the concrete. The specimens exposed to sodium sulphate solutions were most degraded. Thernardite crystals (white and soft) were formed, while epsomite (hard and light grey) was found in case of $MgSO_4$ attack. The measuring technique did not allow to quantitatively determine the degradation of these side surfaces. Therefore, it was proposed to use the testing apparatus for accelerated degradation tests in future research regarding sulphate attack in a slightly different way. For specimens which remain in a fixed position the degradation just above the water level can be measured by the laser sensors and the deterioration can be accelerated by brushing at regular intervals.

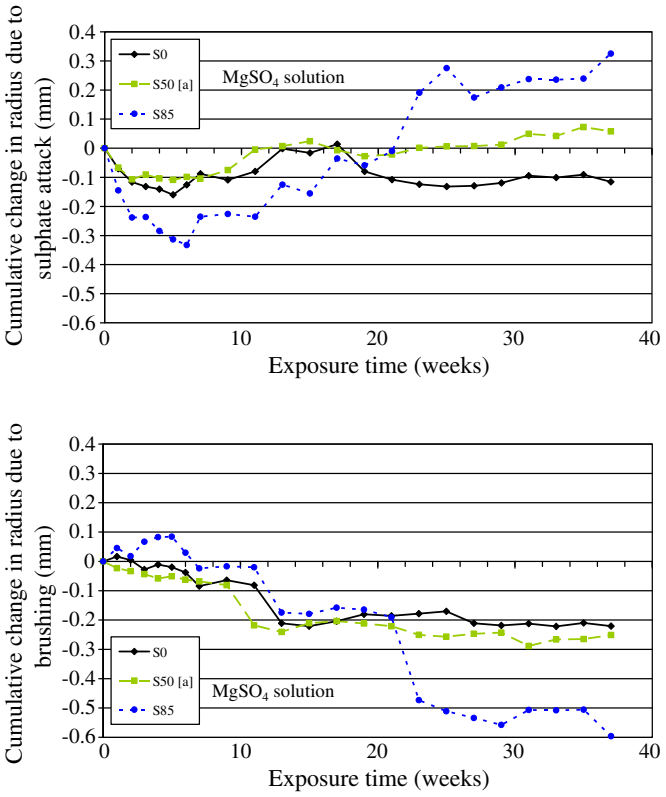

Fig. 18. Cumulative change in radius due to sulphate attack (above) and brushing (below) for test specimens cyclically exposed to a 29.8 g/l $MgSO_4$ solution (S0, S50 [a] and S85).

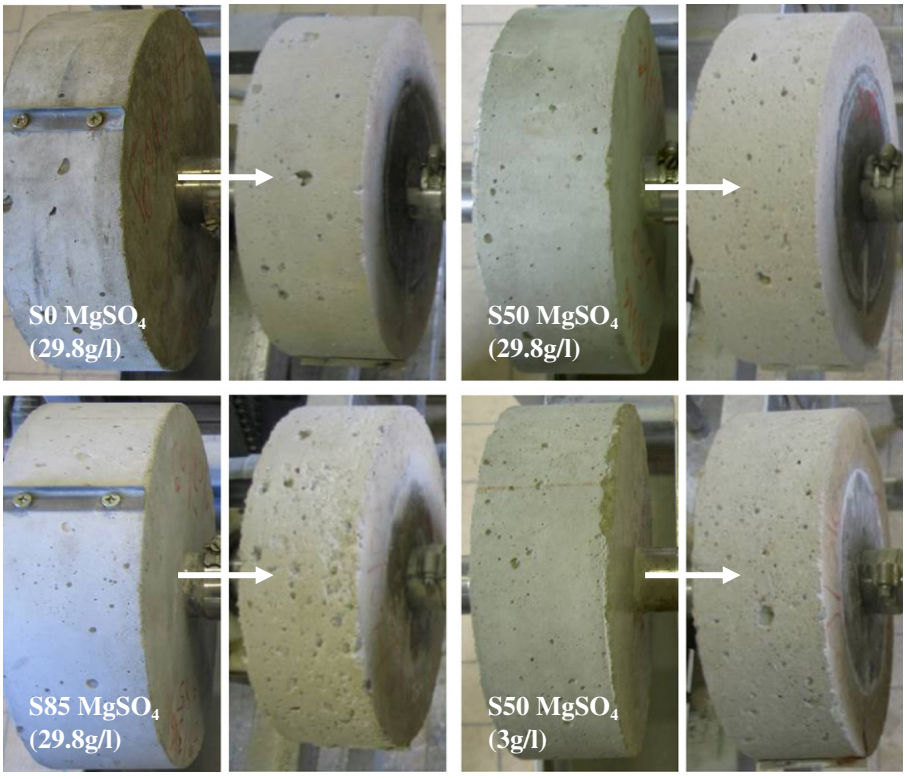

Fig. 17. Image of concrete test specimens before and after 37 weeks cyclical exposure to $MgSO_4$ solutions.

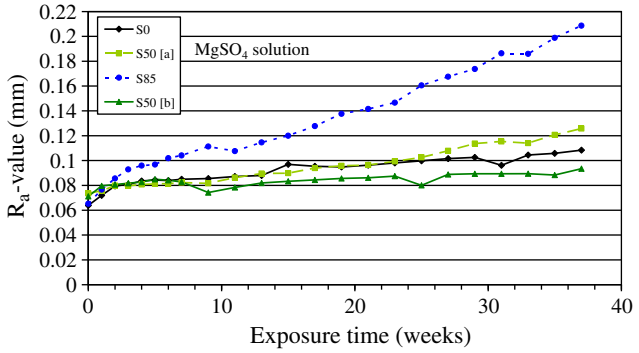

Fig. 19. Evolution of the surface roughness of concrete specimens with different amounts of BFS. The concentration of the $MgSO_4$ solutions was 29.8 g/l for S0, S50 [a] and S85 and 3 g/l for S50 [b].

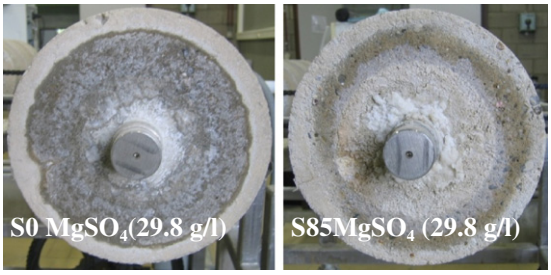

Fig. 20. Crystallisation and degradation of the concrete specimens (exposure time: 37 weeks).

Acknowledgements

As Research Assistant of the Research Foundation-Flanders (FWO-Vlaanderen), the author Elke Gruyaert wants to thank the foundation for the financial support.

References

[1] N. De Belie, J. Monteny, L. Taerwe, Apparatus for accelerated degradation testing of concrete specimens, Mater. Struct. 35 (2002) 427–433.
[2] N. De Belie, Concrete technological and chemical aspects of floor degradation in pig houses, PhD, Univeristy of Ghent, Ghent, 1997.
[3] J. Monteny, Invloed van polymeermodificatie en cementtype op de resistentie van beton tegen chemische en biogene zwavelzuuraantasting PhD, University of Ghent, Ghent, 2002.
[4] A. Bertron, J. Duchesne, G. Escadeillas, Attack of cement pastes exposed to organic acids in manure, Cem. Concr. Compos. 27 (2005) 898–909.
[5] N. De Belie, V. De Coster, D. Van Nieuwenburg, Use of fly ash or silica fume to increase the resistance of concrete to feed acids, Mag. Concr. Res. 49 (1997) 337–344.
[6] J.P. Bayoux, J.P. Letourneux, S. Marcdargent, M. Verschaeve, Acidic Corrosion of High Alumina Cement, Seminar High Alumina Cement, London, 1990.
[7] N. De Belie, M. Debruyckere, D. Van Nieuwenburg, B. De Blaere, Attack of concrete floors in pig houses by feed acids: influence of fly ash addition and cement-bound surface layers, J. Agric. Eng. Res. 68 (1997) 101–108.
[8] A. Bertron, G. Escadeillas, J. Duchesne, Cement pastes alteration by liquid manure organic acids: chemical and mineralogical characterization, Cem. Concr. Res. 34 (2004) 1823–1835.
[9] N. De Belie, R. Verschoore, D. Van Nieuwenburg, Resistance of concrete with limestone sand or polymer additions to feed acids, Trans. ASAE 41 (1998) 227–233.
[10] N. De Belie, H.J. Versnelder, B. De Blaere, D. Van Nieuwenburg, R. Verschoore, Influence of the cement type on the resistance of concrete to feed acids, Cem. Concr. Res. 26 (1996) 1717–1725.
[11] A. Bertron, J. Duchesne, G. Escadeillas, Accelerated tests of hardened cement pastes alteration by organic acids: analysis of the pH effect, Cem. Concr. Res. 35 (2005) 155–166.
[12] Z. Liu, Study of the basic mechanisms of sulfate attack on cementitious materials, PhD, University of Ghent and Central South University, 2010.
[13] B. Tian, M.D. Cohen, Does gypsum formation during sulfate attack on concrete lead to expansion? Cem. Concr. Res. 30 (2000) 117–123.
[14] R. El-Hachem, E. Rozière, F. Grondin, A. Loukili, Influence of sulphate solution concentration on the performance of cementitious materials during external sulphate attack, in: M.G. Alexander, A. Bertron (Eds.), Concrete in Aggressive Aqueous Environments, Performance, Testing and modeling, RILEM publications SARL, Toulouse, France, 2009.
[15] M. Santhanam, M.D. Cohen, J. Olek, Effects of gypsum formation on the performance of cement mortars during external sulfate attack, Cem. Concr. Res. 33 (2003) 325–332.
[16] T. Schmidt, B. Lotenbach, M. Romer, J. Neuenschwander, K.L. Scrivener, Physical and microstructural aspects of sulfate attack on ordinary and limestone blended Portland cements, Cem. Concr. Res. 39 (2009) 1111–1121.
[17] N. Crammond, The occurence of thaumasite in modern construction — a review, Cem. Concr. Compos. 24 (2002) 393–402.
[18] H.A.F. Dehwah, Effect of sulfate concentration and associated cation type on concrete deterioration and morphological changes in cement hydrates, Constr. Build. Mater. 21 (2007) 29–39.
[19] D.D. Higgins, Increased sulfate resistance of ggbs concrete in the presence of carbonate, Cem. Concr. Compos. 25 (2003) 913–919.
[20] J. Skalny, J. Marchand, I. Odler, Sulphate Attack on Concrete, Spon press, New York, 2002.
[21] F. Türker, F. Aköz, S. Koral, N. Yüzer, Effects of magnesium sulfate concentration on the sulfate resistance of mortars with and without silica fume, Cem. Concr. Res. 27 (1997) 205–214.
[22] M. Santhanam, M.D. Cohen, J. Olek, Mechanism of sulfate attack: a fresh look. Part 2. Proposed mechanisms, Cem. Concr. Res. 33 (2003) 341–346.
[23] P.W. Brown, R.D. Hooton, B.A. Clark, Microstructural changes in concretes with sulfate exposure, Cem. Concr. Compos. 26 (2004) 993–999.
[24] H. Taylor, Cement Chemistry, 2nd edition Thomas Telford Publishing, London, 1997.
[25] E. Rozière, A. Loukili, R. El Hachem, F. Grondin, Durabiltiy of concrete exposed to leaching and external sulphate attacks, Cem. Concr. Res. 39 (2009) 1188–1198.
[26] AFPC-AFREM, Recommended test methods for measuring the parameters associated to durability (in French), Proc of Journées Techniques AFPC-AFREM 'Durabilité des Bétons', Toulouse, 1998.
[27] K. Audenaert, Transportmechanismen in zelfverdichtend beton in relatie met carbonatatie en chloridepenetratie, PhD, Ghent University, Ghent, 2006.
[28] V. Cnudde, A. Cwirzen, B. Masschaele, P.J.S. Jacobs, Porosity and microstructure characterization of building stones and concretes, Eng. Geol. 103 (2009) 76–83.
[29] E.P. Kearsley, P.J. Wainwright, Porosity and permeability of foamed concrete, Cem. Concr. Res. 31 (2001) 805–812.
[30] RILEM, Tests defining the structure — porosity accessible to water, Mater. Struct. 13 (1980) 177–178.
[31] P. Van den Heede, E. Gruyaert, N. De Belie, Transport properties of high-volume fly ash concrete: capillary water sorption, water sorption under vacuum and gas permeability, Cem. Concr. Compos. 32 (2010) 749–756.
[32] A. Peschard, A. Govin, P. Grosseau, B. Guilhot, R. Guyonnet, Effect of polysaccharides on the hydration of cement paste at early ages, Cem. Concr. Res. 34 (2004) 2153–2158.
[33] D.S. Klimesch, A. Ray, The use of DTA/TGA to study the effects of ground quartz with different surface areas in autoclaved cement: quartz pastes. Part 1: A method for evaluating DTA/TGA results, Thermochim. Acta 289 (1996) 41–54.
[34] P.H.R. Borges, J.O. Costa, N.B. Milestone, C.J. Lynsdale, R.E. Streatfield, Carbonation of CH and CSH in composite cement pastes containing high amounts of BFS, Cem. Concr. Res. 40 (2010) 284–292.
[35] G. Baert, Physico-chemical interactions in Portland cement-(high volume) fly ash binders, PhD, Ghent University, Ghent, 2009.
[36] J.I. Escalante-Garcia, J.H. Sharp, Effect of temperature on the hydration of the main clinker phases in Portland cements: part II, blended cements, Cem. Concr. Res. 28 (1998) 1259–1274.
[37] J. Stark, B. Möser, F. Bellmann, Nucleation and growth of C–S–H phases on mineral admixtures, in: C.U. Grosse (Ed.), Advances in Construction Materials, Springer, Berlin, 2007, pp. 231–538.
[38] E. Gruyaert, Effect of Blast-Furnace Slag as Cement Replacement on Hydration, Microstructure, Strength and Durability of Concrete, PhD, University of Ghent, Ghent, 2011.
[39] P.C. Hewlett, Lea's Chemistry of Cement and Concrete, Elsevier, London, 1998.
[40] J. Zhou, G. Ye, K. Van Breugel, Hydration of Portland cement blended with blast furnace slag at early age, in: J. Marchand, B. Bissonnette, R. Gagné, M. Jolin, F. Paradis (Eds.), Second International Symposium on Advances in Concrete through Science and Engineering, Québec, 2006, (pp. CD-ROM).
[41] C. Shi, J.A. Stegemann, Acid corrosion resistance of different cementing materials, Cem. Concr. Res. 30 (2000) 803–808.
[42] W. Chen, H.J.H. Brouwers, The hydration of slag, part 2: reaction models for blended cement, J. Mater. Sci. 42 (2007) 444–464.
[43] I. Biczok, Concrete Corrosion Concrete Protection, Chemical Publishing Company Inc., New York, 1967.
[44] M.D. Cohen, B. Mather, Sulfate attack on concrete — research needs, ACI Mater. J. 88 (1991) 62–69.
[45] K. Van Tittelboom, N. De Belie, A critical review on test methods for evaluating the resistance of concrete against sulfate attack, Concrete in Aggressive Aqueous Environments: Performance, Testing and Modeling, RILEM publications SARL, Toulouse, France, 2009, pp. 298–306.
[46] Z. LIu, D. Deng, G. De Schutter, Z. Yu, Micro-analysis of "salt weathering" on cement paste, Cem. Concr. Compos. 33 (2011) 179–191.
[47] Z. Liu, G. De Schutter, D. Deng, Z. Yu, Micro-analysis of the role of interfacial transition zone in "salt weathering" on concrete, Constr. Build. Mater. 24 (2010) 2052–2059.
[48] Verein Deutscher Zement Werke (VDZ), Testing of sulfate resistance of cement with small and flat prisms and according to the original procedure of Koch/Steinegger and Wittekindt, , 1996.
[49] Verein Deutscher Zement Werke (VDZ), Prüfung des Sulfatwiderstands von Zement nach dem Wittekindt, SVA und CEN-Verfahren, , 2002.